Numerical Simulation of Silicon Laser Ablation with GHz Bursts of Femtosecond Pulses

Ashkan Momeni and Koji Sugioka*

RIKEN Center for Advanced Photonics, 2-1 Hirosawa, Wako-shi, Saitama 351-0198, Japan
**Corresponding author's e-mail: ksugioka@riken.jp*

We simulate laser ablation of silicon with GHz bursts of femtosecond laser pulses using COMSOL Multiphysics. The simple model of deformation geometry is considered to simulate laser ablation and material removal, giving a laser-induced crater after irradiation. We demonstrate that at the same burst pulse energy a deeper crater is ablated for a GHz burst for larger number of intra-pulses. Analysis of the temperature evolution of silicon target reveals that during femtosecond laser irradiation with GHz burst mode, efficient absorption of laser energy occurs due to the heat-accumulation effect. These simulated results show a good agreement with the experimental measurements and could quantitatively explain the mechanism of silicon ablation enhancement with the GHz bursts of femtosecond laser pulses.
DOI: 10.2961/jlmn.2023.02.2010
Keywords: ablation, femtosecond laser, GHz burst-mode, micro-machining, silicon

1. Introduction

Femtosecond laser processing with high quality and high efficiency has received great attention for commercial applications [1-3]. In the last decade, many research efforts have focused on improving the efficiency of laser-induced microfabrication by using bursts of femtosecond pulses [4-10]. In this context, we investigated the femtosecond laser processing of silicon by utilizing the GHz burst mode and GHz bursts in MHz bursts (BiBurst) mode to improve the ablation yield [9, 10]. The experimental results indicated that the GHz burst mode laser ablation of silicon can produce deeper craters compared with ablation by the conventional irradiation scheme of a series of single pulses (single-pulse mode) at the same total energy deposited on the target [7-10]. The ablation enhancement can be conceptually described by efficient absorption of the subsequent laser pulses in the GHz burst by free electrons excited by the preceding laser pulses and the heat-accumulation effect [7-10]. However, to the best of our knowledge, the possible mechanisms have not yet been completely understood, which encourages us to investigate it in more detail.

Recently, many research efforts have been carried out in simulation of silicon laser processing, mainly on the two-temperature model to describe the heating and ablation during ultrafast laser irradiation [6, 11-13]. However, prediction of the ablation efficiency using this model requires a precise analysis of the isotherm distribution of material to determine the best isotherm which should be similar to the experimental crater profile [13]. This analysis is particularly difficult and challenging to simulate laser ablation in burst mode with multiple laser pulses. In the present study, we simulated the GHz burst mode femtosecond laser ablation of silicon by using COMSOL Multiphysics. The simple model of deformation geometry enabled us to simulate profiles of the laser-produced craters as well as the temperature evolution of silicon target during the laser processing. We carried out the simulation with the same laser irradiation parameters as the experiments to compare the simulation results with the experimental data published in our previous work [9]. The simulated results were in a good agreement with the experimental ones to show enhancement of silicon ablation efficiency with the GHz burst mode femtosecond laser processing. To investigate the underlying mechanisms of the ablation efficiency enhancement, the temperature evolution of silicon target during the irradiation process was evaluated. This analysis confirmed that the heat-accumulation effect and efficient absorption of laser energy are responsible for higher efficiency in ablation by the GHz burst mode laser processing.

2. Simulation method

Simulation of the laser ablation process was conducted using COMSOL Multiphysics software based on the finite element method. The model of deformation geometry was applied to investigate the material removal and ablation depth. Figure 1 shows a two-dimensional axisymmetric geometry that was considered for silicon with a thickness of 5 μm and a diameter of 20 μm in axial and radial directions, respectively.

The absorbed laser energy of a single burst pulse, which consisted of a train of femtosecond laser pulses (up to 25 pulses) at a wavelength of 1030 nm with an interval of 205 ps corresponding to 4.88 GHz, was assumed as an incoming heat flux on the silicon surface. We defined the laser intensity of the GHz burst pulse as [13]:

$$I(r,z,t) = (1-R)\left(\frac{2E_{Burst}}{\pi\omega^2}\right)B(t)\, e^{-2\left(\frac{r}{\omega}\right)^2} e^{\alpha(z-z_0)} \quad (1)$$

where R is the reflectivity of silicon, E_{Burst} is the burst pulse energy and ω is the focused laser spot radius on the surface of silicon. Moreover, $\alpha = \alpha_{SPA} + \alpha_{FCA}$ stands for sum of the coefficients of inter-band absorption by a single-photon and native free carrier absorption [13].

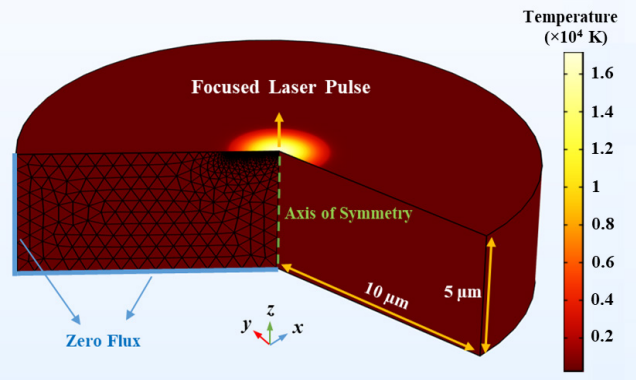

Fig. 1 Computational geometry for silicon with a thickness of 5 μm and a diameter of 20 μm. The left-hand side of cross-section shows the mesh structures as well as the boundary conditions. The laser pulse was considered as a heat flux at the top surface of silicon, whereas zero flux boundary conditions were applied to the left and bottom boundaries (blue lines). The color bar represents the value of temperature in K.

The function of *B(t)* represents the laser energy distribution of the GHz burst pulse over time defined by [6]:

$$B(t)=\frac{1}{\tau}\sqrt{\frac{4\ln 2}{\pi}}\left[\frac{1}{P}\sum_{n=0}^{P-1}e^{-4\ln 2\left(\frac{t-(n\Delta t+t_0)}{\tau}\right)^2}\right] \quad (2)$$

with τ being the pulse width of 220 fs, P the number of pulses in a GHz burst (intra-pulse number) and Δt the time separation between intra-pulses (205 ps). Figure 2(a) depicts the temporal distribution of laser energy for a single GHz burst pulse with P = 10 which consists of a train of 10 identical intra-pulses at a repetition rate of 4.88 GHz. It should be noted that the peak of function *B(t)* is normalized to 1 for single-pulse mode (P = 1) and GHz burst mode with different P. Moreover, the laser energy is evenly distributed over the intra-pulses in the GHz burst pulse. Therefore, for the GHz burst pulse with P = 10 the maximum value for each intra-pulse in the burst is 1/10.

By considering the GHz burst of femtosecond laser pulses as a heat source, the model of heat transfer through thermal conduction was used to obtain the temperature evolution of silicon during the irradiation process. The heat transfer model can be expressed by [14]:

$$\rho C(T)\frac{\partial T}{\partial t}-\nabla\cdot(k\nabla T)=0 \quad (3)$$

in which ρ and k are the density and thermal conductivity of silicon, respectively. In this equation *C(T)* represents the silicon specific heat capacity as a function of temperature, given by [15]:

$$C(T)=783.3+(0.1017)T-(9.77\times10^{-6})T^2$$
$$300\le T\le 1683 \quad (4)$$

It should be noted that the energy lost by the thermal convection and thermal radiation was ignored in simulations because of the dominant absorption of laser energy by the material [13].

As Figure 1 shows, the GHz burst pulse was applied as a boundary heat flux at the surface of silicon defined by [16]:

$$-\mathbf{n}\cdot(k\nabla T)=I(r,z,t) \quad (5)$$

where $\boldsymbol{n}$ is the normal vector of surface. However, for other boundaries the thermal insulation and zero flux boundary conditions were assumed. The overall computational geometry was discretized using a triangular coarse mesh, while a finer mesh was employed in the region near the laser heat source to improve the spatial resolution [17]. To simulate the material removal using the deformation geometry technique, the energy balance at the surface of silicon was considered and the normal mesh velocity was determined by [16, 17]:

$$\boldsymbol{v}_{mesh}\cdot\mathbf{n}=v_{vap}=\frac{\Phi_{vap}}{\rho L_v} \quad (6)$$

where v_{vap} is the vaporization velocity, L_v denotes the latent heat of evaporation and ρ is the density of silicon. In this equation, the ablative heat flux Φ_{vap} can be expressed as [16, 17]:

$$\Phi_{vap}=h(T-T_v) \quad (7)$$

with T_v being the vaporization temperature and h an effective heat transfer coefficient defined by a ramp function. This ablative heat flux can result in a deformed geometry due to the surface temperature exceeding the vaporization threshold and thereby can describe the material removal. In order to provide comparable results, an optimized heat transfer coefficient was determined by a best fit of the simulation result to the measured experimental data for single-pulse mode at the pulse energy of 0.1 μJ. Then, this optimized parameter was used in the simulation of laser ablation process for a GHz burst pulse with different intra-pulse numbers and different burst energies. The values of parameters used in the simulation including laser parameters, optical and thermal properties of silicon are summarized in Table 1.

Table 1 Parameters used in simulation of the laser ablation process.

Symbol	Parameter	Value
ω	Spot size radius	1.9 μm
τ	Pulse width	220 fs
Δt	Time between intra-pulses	205 ps (4.88 GHz)
t_0	Peak time of the Gaussian pulse	880 fs (4τ)
z_0	Surface position of silicon	5 μm
R	Reflectivity	0.329
α	Absorption coefficient	2.2348×10^6 1/m
ρ	Density	2330 kg/m^3
C(T)	Heat capacity	Eq (4) J/kg K
k	Thermal conductivity	148 W/m K
T_v	Ablation temperature	3538 K
T_{in}	Initial temperature	300 K
L_v	Latent heat of evaporation	1.28×10^7 J/kg
h	Heat transfer coefficient	10^7 W/m^2 K

3. Result and discussion

Figure 2 shows the simulation results of silicon laser ablation and crater formation by using a single GHz burst pulse with P = 10 at the burst pulse energy of 0.1 μJ. As Figure 2(c) shows, by each intra-pulse irradiation, the temperature of silicon could reach the vaporization point to ablate silicon. Moreover, the black marked points in Fig. 2(c) indicate the temperatures at the point A in Fig. 2 (b) at the start time of irradiation of each intra-pulse. These results clearly reveal that the subsequent intra-pulses contributed to a gradual increase of temperature in the silicon due to heat accumulation effect [7]. This may result in an efficient absorption of the laser energy because the absorption coefficient of silicon can increase with temperature [18, 19].

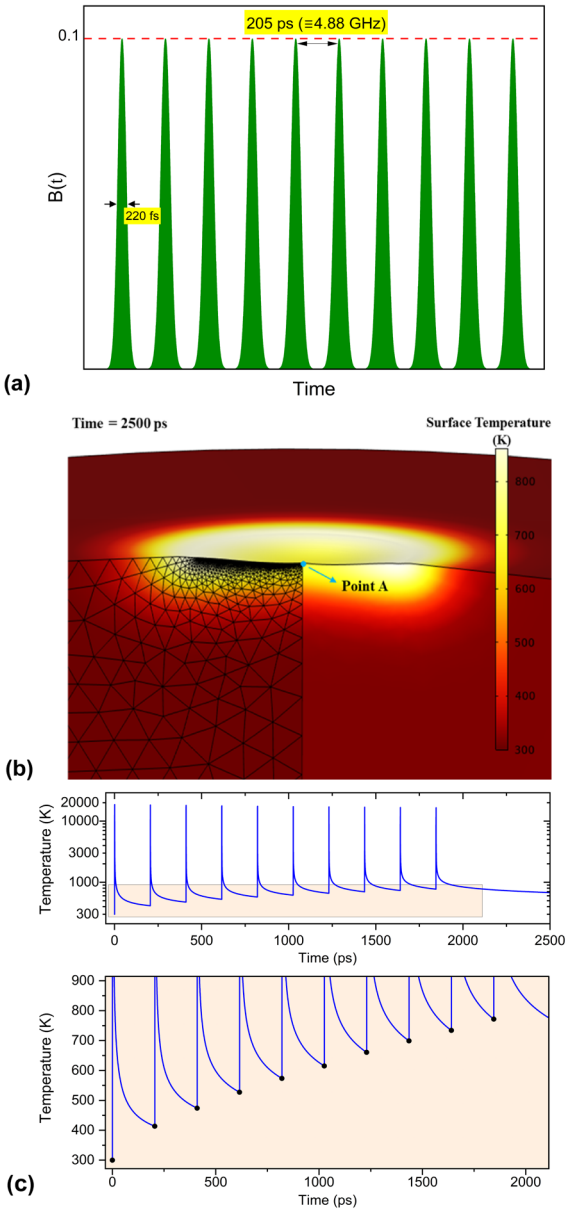

Fig. 2 (a) A pulse shape of a single burst of femtosecond laser pulses with P = 10 with a burst pulse energy of 0.1 μJ at a 4.88 GHz repetition rate. (b) Simulation of silicon laser ablation by this GHz burst. The central point of laser spot is shown by point A. The color bar represents the value of temperature in K. (c) Temperature evolution of silicon (Point A in (b)) by the irradiation of a single burst pulse. The temperatures at the point A at the start time of irradiation of each intra-pulse are shown by the black marked points in the lower figure which enlarges the pink color regions in the upper figure.

The laser ablation process was simulated for GHz bursts with different P from 1 (single-pulse mode), to 2, 10, 20, and 25 at different burst energies of 0.1, 0.2 and 0.3 μJ. As Figure 3 shows, the results indicated that at the same burst pulse energy a deeper crater was ablated for a GHz burst with larger P. The numerical results were in good agreement with the experimental measurements for P = 10 and smaller, demonstrating enhancement of silicon ablation efficiency with the GHz bursts of femtosecond laser pulses. However, for P = 20 and 25, there were some differences between the simulation and experimental results. Specifically, the simulation results are smaller than the experimental results, and the difference decreases with increasing the burst energy from 0.1 to 0.3 μJ.

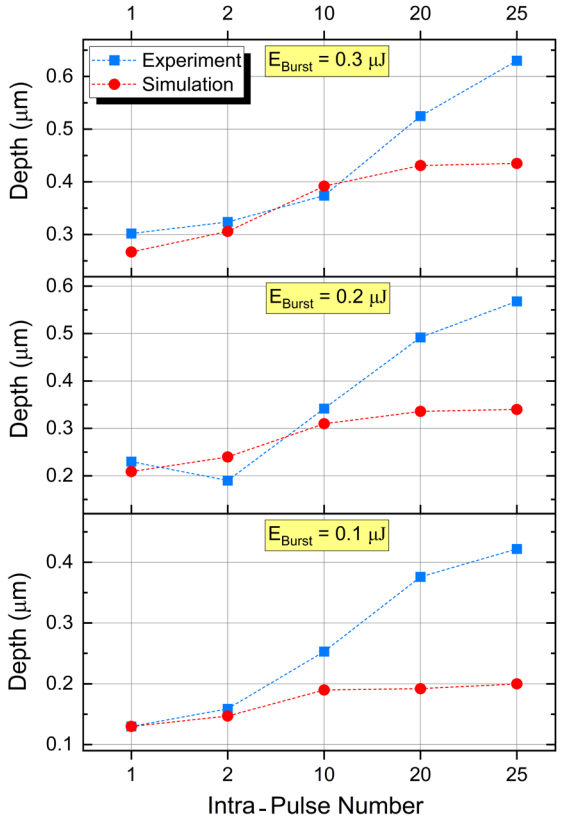

Fig. 3 Comparison of the experimental and simulated ablation depths for GHz bursts of femtosecond laser pulses with different intra-pulse numbers of P = 1, 2, 10, 20, and 25 at different burst energies of 0.1, 0.2 and 0.3 μJ.

To identify the cause of these differences, we investigated the evolution of temperatures at the point A in Fig. 2 (b) of silicon target when each intra-pulse was irradiated, and the corresponding results for the burst energies of 0.1 and 0.3 μJ were presented in Figure 4. For the GHz burst mode laser ablation with P = 2 and 10 at the burst pulse energy of 0.1 μJ, silicon temperature at the start time of irradiation of each intra-pulse (black marked points in the lower of Fig. 2 (c)) gradually increases up to about 420 and 770 K, respectively (see Figure 4(a)). Meanwhile, for the bursts with P = 20 and 25, after the 10th intra-pulse irradiation the temperature increases more significantly due to the heat accumulation effect. As Figure 4(a) shows, the temperatures of silicon at the start time of irradiation of last

intra-pulses were about 1150 and 1296 K when the 20th and 25th intra-pulses were irradiated on the target, respectively (see arrow signs in Fig. 4(a)). This can be explained by the different laser energy transfer during irradiation of the GHz bursts with different P. In fact, a GHz burst pulse with a larger P has a lower energy level for each intra-pulse ($B(t) \propto 1/p$). Based on Eqs. (3) and (5), a lower energy intra-pulse could result in a lower temperature gradient and a lower rate of temperature change over time. It should be noted that the corresponding temperatures for higher GHz burst energy of 0.3 μJ are lower than those for 0.1 μJ. Since a higher temperature gradient can be achieved by increasing the energy of burst pulse, resulting in a higher heat transfer rate. For this reason, during each intra-pulse irradiation the temperature was changed at a higher rate to give rise to the improved ablation efficiency.

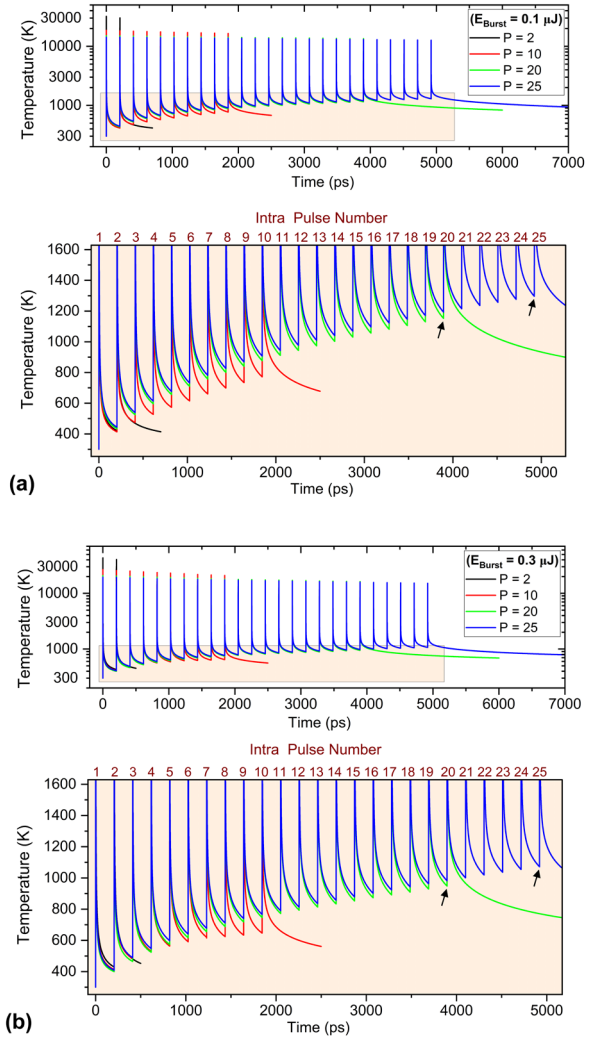

Fig. 4 Temperature evolution of silicon in the GHz burst mode laser ablation with P = 2, 10, 20, and 25 when each intra-pulse was irradiated on the target for burst energies of (a) 0.1 and (b) 0.3 μJ. The lowers are an enlargement of the pink area in the upper figures.

We further simulated the ablation depth at larger burst pulse energy to compare the experimental results. Figure 5 shows the simulated ablation depth versus burst pulse energy for the GHz burst with P = 25. As this figure shows, the ablation depth of silicon increases as the burst pulse energy increases. We quantitatively obtained a good agreement with the experimental results for ablation depth as well as crater profile on silicon (see Figure 6), and better agreement was achieved at larger burst pulse energy. This may be caused by different temperature changes of silicon during the ablation process. As can be seen in Figure 7, the temperature evaluation analysis revealed that the rate of silicon temperature rise decreased with an increase in the burst energy from 0.1 to 1 μJ. The magnitude of silicon temperature at the start time of last intra-pulse in the burst with P = 25 was decreased to approximately 880 K for the burst energy of 1 μJ from 1296 K for 0.1 μJ energy (see arrow sign in Fig. 7(a)). This was also demonstrated by considering the temperature evolution at the deepest points of ablated surfaces which was presented in Figure 7(b).

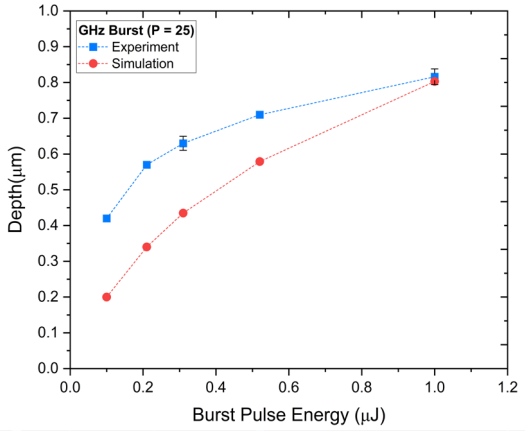

Fig. 5 Comparison of the experimental and simulated ablation depths for a GHz burst with intra-pulse number of P = 25 at different burst energies. The error bars show standard deviations for experimental data at the burst energies of 0.3 μJ and 1 μJ.

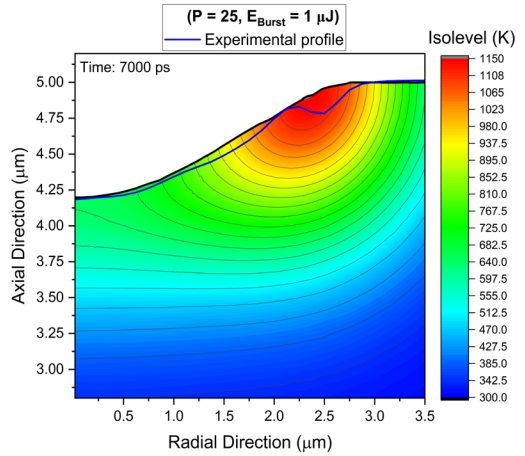

Fig. 6 Cross-sectional view of a simulated crater with corresponding isotherm curves formed by a GHz burst with P = 25 and burst pulse energy of 1 μJ. The experimental result is also shown with a blue solid line.

These results suggested that the difference between simulation and experimental results could be due to the temperature dependence of absorption coefficient. Indeed, we defined a constant absorption coefficient for silicon in the simulation. However, the absorption coefficient of silicon could increase with temperature up to its melting point (1638 K), especially for temperatures exceeding 1000 K.

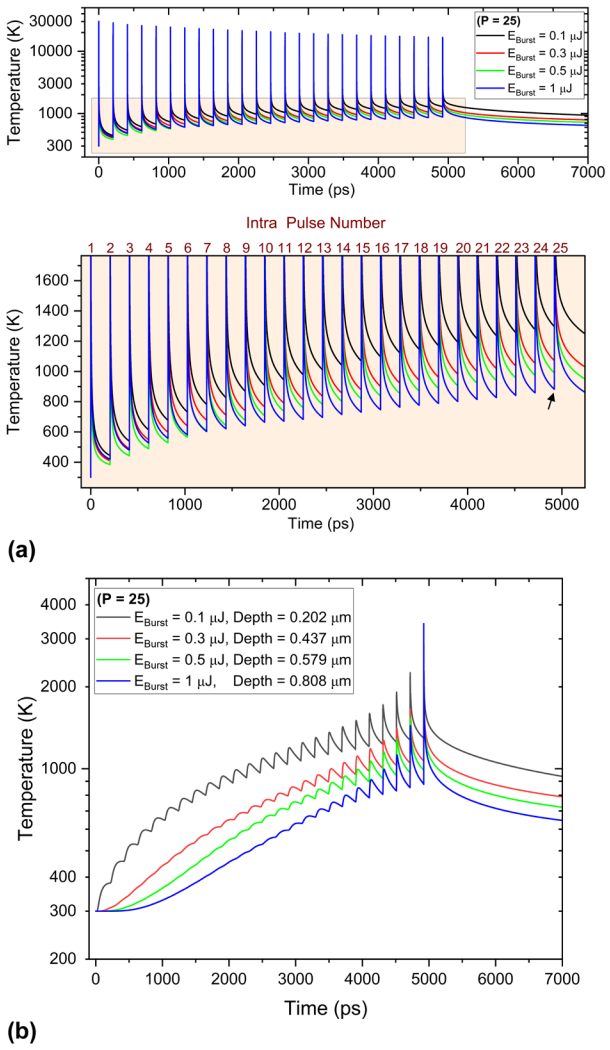

Fig. 7 (a) Evolution of temperature increase rate of silicon at (a) the point A and (b) the deepest points of ablated surfaces by a GHz burst with P = 25 at the burst energies from 0.1 to 1 μJ.

This was confirmed by a theoretical model predicting the absorption coefficient of silicon as a function of temperature at the wavelength of 1064 nm as described by [19]:

$$\alpha = 12.991 \exp(4.8 \times 10^{-3}\, T) - 52.588 \exp(-2.3 \times 10^{-4}\, T) \quad (8)$$

where T is temperature. Based on this model, as shown in Figure 8, the absorption coefficient of silicon would increase significantly with temperature and should be considered for more precise interpretation of results. There are no data on temperature dependence of absorption coefficient at the wavelength of 1030 nm available. It is, however, expected that the absorption coefficient of silicon at 1030 nm would increase with temperature similar to that found for 1064 nm, since both the wavelengths of 1064 nm (1.16 eV) and 1030 nm (1.2 eV) are close to the indirect bandgap of silicon (1.12 eV) [9]. Another possibility for the increase of absorption coefficient is absorption of the subsequent intra-pulses in the burst by free electrons generated by the preceding intra-pulses, as we previously suggested [9, 10]. However, the lager pulse energy can generate more free electrons which should induce larger absorption. This fact cannot explain the discrepancy between the experimental and simulation results at lower burst pulse energy shown in Fig. 5. Therefore, the increase of absorption coefficient by temperature increase may be more likely to explain the discrepancy.

Therefore, it could be concluded that the enhancement of ablation efficiency of silicon in the GHz burst mode laser processing was more dominantly originated from the efficient absorption of subsequent laser pulses in the GHz burst because of the heat-accumulation effect. Especially, for GHz burst with larger P of 20 and 25 the temperature dependence of silicon absorption coefficient could be expected to play significant role in the absorption of laser energy and ablation enhancement.

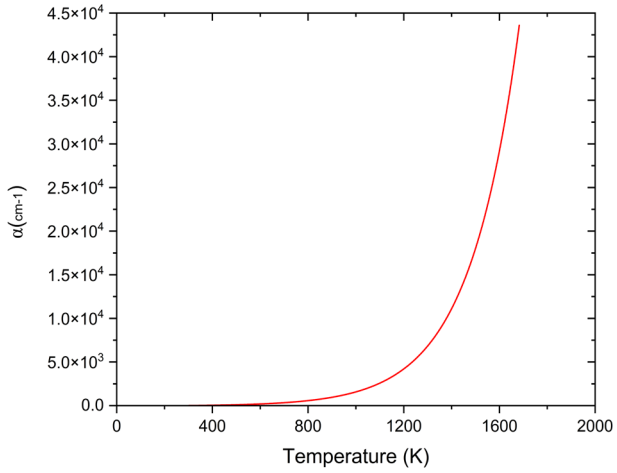

Fig. 8 Temperature dependence of absorption coefficient of silicon.

4. Conclusion

This study presented a numerical simulation of the GHz burst mode femtosecond laser ablation of silicon with different number of intra-pulses using COMSOL Multiphysics. The simple model of deformation geometry predicted the ablation depth as well as profiles of the laser-induced craters with a quantitatively good agreement with the experimental measurements. The results demonstrated that laser ablation of silicon with the GHz bursts of femtosecond pulses could improve the ablation yield. Analysis of the temperature evaluation of silicon revealed that the ablation enhancement was more dominantly originated from efficient absorption of subsequent intra-pulses in the GHz burst because of the heat-accumulation effect. In this context, temperature dependence of silicon absorption coefficient may play major role in the efficient absorption of laser energy for GHz bursts with high intra-pulse numbers.

Acknowledgments and Appendixes

This work was partially supported by MEXT Quantum Leap Flagship Program (MEXT Q-LEAP) Grant Number JPMXS0118067246.

References

[1] K. Sugioka: Int. J. Extrem. Manuf., 1, (2019) 012003.
[2] B. Guo, J. Sun, Y. Hua, N. Zhan, J. Jia, and K. Chu: Nanomanuf Metrol., 3, (2020) 26.

[3] Z. Lin and M. Hong: Ultrafast Sci., 2021, (2021) 1.
[4] K. Obata, F. Caballero-Lucas, and K. Sugioka: J. Laser Micro/Nanoeng., 16, (2021)19.
[5] A. Žemaitis, M. Gaidys, P. Gečys, M. Barkauskas, and M. Gedvilas: Opt. Express, 29, (2021) 7641.
[6] C. Gaudiuso, P. N. Terekhin, A. Volpe, S. Nolte, B. Rethfeld, and A. Ancona: Sci Rep, 11, (2021) 13321.
[7] K. Mishchik, G. Bonamis, J. Qiao, J. Lopez, E. Audouard, E. Mottay, C. Hönninger, and I. Manek-Hönninger: Opt. Lett., 44, (2019) 2193.
[8] G. Bonamis, E, Audouard, C. Hönninger, J. Lopez, K. Mishchik, E. Mottay, and I. Manek-Hönninger: Opt. Express, 28, (2020) 27702.
[9] F. Caballero-Lucas. K. Obata, and K. Sugioka: Int. J. Extrem. Manuf., 4, (2022) 015103.
[10] K. Obata, F. Caballero-Lucas, Sh. Kawabata, G. Miyaji, and K. Sugioka: Int. J. Extrem. Manuf., 5, (2023) 025002.
[11] L. L. Taylor, R. E. Scott, and J. Qiao: Opt. Mater. Express, 8, (2018) 648.
[12] R. Moser, M. Domke, J. Winter, H. P. Huber, and G. Marowsky: Adv. Opt. Techn., 7, (2018) 255.
[13] C. Chen, F. Zhang, Y. Zhang, X. Xiong, B. F. Ju, H. Cui, and Y. L. Chen: Appl. Surf. Sci, 576, (2022) 151722.
[14] L. Gallais, T. Vidal, E. Lescoute, Y. Pontillon, and J. L. Rullier: J. Appl. Phys., 129, (2021) 043102.
[15] R. K. Endo, Y. Fujihara, and M. Susa: High Temp. High Press, 35, (2003) 5.
[16] E. C. Chevallier, V. Bruyere, G. Bernard, and P. Namy, Femto-second laser texturing prediction using COMSOL Multiphysics®.
[17] L. Peng, M. Li, P. Wang, M. He, C. Zhou, H. Zhang, and S. Chen, Available at SSRN 4280222.
[18] A. Rämer, O. Osmani, and B. Rethfeld: J. Appl. Phys., 116, (2014) 053508.
[19] E. Ohmura: "Heat Transfer-Engineering Applications" ed. by V. Vikhrenko, (Publisher, Intech, 2011) p.32.

(Received: June 10, 2023, Accepted: September 15, 2023)